Synthesis, characterisation and biological properties of gold(III) compounds with modified bipyridine and bipyridylamine ligands†

Angela Casini,* Mariam Celine Diawara, Rosario Scopelliti, Shaik Mohammed Zakeeruddin, Michael Grätzel and Paul J. Dyson

Received 7th October 2009, Accepted 20th November 2009
First published as an Advance Article on the web 7th January 2010
DOI: 10.1039/b921019a

Square planar gold(III) complexes that contain functionalised bipyridine ligands of general formula $[Au(N\wedge N)Cl_2][PF_6]$ [where N∧N = 2,2′-bipyridine, 4,4′-dimethyl-2,2′-bipyridine, 4,4′-dimethoxy-2,2′-bipyridine and 4,4′-diamino-2,2′-bipyridine] have been prepared and characterised by NMR spectroscopy and mass spectrometry. Two of the complexes have also been characterised in the solid state by X-ray crystallography. In addition, a gold(III) compound bearing a dipyridin-2-ylamine ligand was also prepared and characterised. The complexes were found to undergo hydrolysis under pseudo-physiological conditions. Moreover, the complexes showed moderate to good cytotoxicity *in vitro* towards the A2780 human ovarian carcinoma cell line and the cisplatin resistant variant A2780cisR. Reactivity studies with biomolecules, such as reducing agents, plasmid DNA and a model protein (ubiquitin) were also performed to provide tentative insights into the mode of action of the complexes.

Introduction

In the last decade a number of gold(III) compounds that are highly cytotoxic towards cancer cells have been discovered.[1,2,3,4] Indeed, various classes of gold(III) compounds have been prepared and characterised that are stable under physiological-like conditions and manifest significant antiproliferative properties *in vitro*, including gold dithiocarbamates,[5] gold porphyrins,[6,7] dinuclear gold complexes,[8] and a variety of organogold compounds.[9,10] Most of the above compounds are not only strongly cytotoxic, but they are also able to overcome cisplatin resistance. In addition to *in vitro* studies, *in vivo* tumour growth inhibition by gold(III) compounds has been demonstrated.[11,12]

Studies indicate that gold(III) compounds produce their antiproliferative effects through non-conventional modes of action.[13,14] For instance, the hypothesis that their biological effects are mediated by an antimitochondrial mechanism rather than by direct DNA damage has gained much credit.[14] Very recently, *COMPARE* analysis of cancer cell growth inhibition data of a panel of gold(III) compounds in comparison to 110 standard agents with known mechanisms of action suggested that numerous and heterogeneous molecular mechanisms are involved, including inhibition of cyclin-dependent kinases or histone deacetylases.[15]

Within this frame, we have synthesised some novel gold(III) compounds, whose chemical structures are schematically represented in Scheme 1. These structures were inspired by previous work in the field and by some initial structure–activity correlations that were formerly proposed.[16] In particular, bipyridyl gold(III) compounds developed by Cinellu *et al.*, *e.g.* $[Au(bipy)(OH)_2][PF_6]$ (bipy = 2,2′-bipyridine) (Aubipy),[17] show particular promise. They possess good stability under physiological-like conditions and exhibit excellent cytotoxic properties towards certain human cancer cell lines.[18] Moreover, a subsequent study describing a series of oxo-bridged dinuclear gold(III) compounds with substituted 2,2′-bipyridines[19] drew initial structure–activity relationships relating the electronic effects of different substituents at the 6,6′-positions with the cytotoxic activities. Notably, the 6,6′-dimethyl-2,2′-bipyridine derivative showed the most pronounced antiproliferative effects paired with peculiar structural and redox properties among the members of the series.

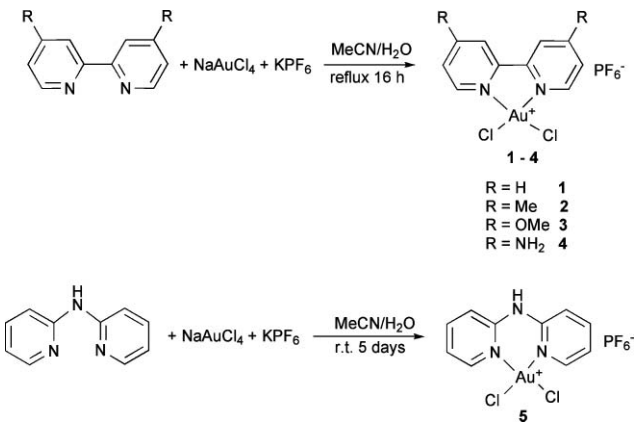

Scheme 1 Synthesis of **1**–**5**.

Inspired by these promising results, we have synthesised the chloride precursor of Aubipy, *i.e.* $[Au(bipy)Cl_2][PF_6]$ (**1**), and novel gold(III) compounds with 4,4′-substituted 2,2′-bipyridine ligands – namely $[Au(bpMe)Cl_2][PF_6]$ (bpMe = 4,4′-dimethyl-2,2′-bipyridine) (**2**), $[Au(bpOMe)Cl_2][PF_6]$ (bpOMe = 4,4′-dimethoxy-2,2′-bipyridine (**3**) and $[Au(bpNH_2)Cl_2][PF_6]$

Institut des Sciences et Ingénierie Chimiques, Ecole Polytechnique Fédérale de Lausanne (EPFL), CH-1015 Lausanne, Switzerland. E-mail: angela.casini@epfl.ch

† Electronic supplementary information (ESI) available: UV-visible spectra and structural information. CCDC reference numbers 750304 and 750305. For ESI and crystallographic data in CIF or other electronic format see DOI: 10.1039/b921019a

(bpNH$_2$ = 4,4′-diamino-2,2′-bipyridine) (**4**) (Scheme 1). The various 2,2-bipyridine ligands were selected in order to investigate the influence of different substituents at the 4,4′-position with different electronic properties on the chemical and biological properties of the resulting complexes, and to compare them with the above mentioned 6,6′-substituted bipyridine compounds. In addition, a closely related gold(III) complex with the dipyridin-2-ylamine (dipyam) ligand [Au(dipyam)Cl$_2$][PF$_6$] (**5**), has been prepared and characterised (Scheme 1). The solution behaviour of the compounds, their *in vitro* antiproliferative effects and reactions with biomolecules such as reducing agents, plasmid DNA and ubiquitin (Ub) are described herein.

Results and discussion

The reference compound for this study, [Au(bipy)Cl$_2$][PF$_6$] **1**, reported by Cinellu *et al.*,[17] was prepared using a modification of the method described fifty years ago by Harris and Lockyer for the perchlorate salt.[20] Compounds **2–4** were prepared using the same method (see Scheme 1), and **5** was synthesised with a modification of a procedure previously reported by Shi and Jiang for [Au(dipyam)Cl$_2$]Cl[21] (Scheme 1). Compounds **1–5** were characterised by NMR spectroscopy and electrospray ionisation mass spectrometry (ESI-MS). Spectroscopic data for **1** is in keeping with that reported previously. ESI-MS of **1–5** in water showed the presence of the expected molecular species and with time partial hydrolysis of the chloride ligands was observed. Compound **5** containing a 2,2′-dipyridylamine ligand, shares some similarities to 2,2′-bipyridine, however the central amine unit introduces important differences: the two pyridine rings of dipyam are flexible in their coordination to metal centres, adopting either nearly coplanar or tilted pyridyl ring planes;[22] ESI-MS analysis of **5** in water revealed a fast hydrolysis and decomposition at 37 °C.

X-Ray analysis

Single crystals of **2** and **3** were obtained in acetonitrile and analysed by X-ray diffraction. Their structures are shown in Fig. 1 and 2, and relevant crystal data for both structures are summarised in Table 1. Both complexes showed, as expected, nearly square-planar geometry at the metal centre (maximum atomic deviation from the least-squares plane < 0.01 Å for **2** and < 0.03 Å for **3**). No apparent steric hindrance is observed within the pyridine rings of the ligands since the dihedral angles between the rings are very close to zero (3.1° for **2** and 4° for **3**). Bond distances around the gold ion are as expected (Au–Cl$_{av}$ = 2.252(4) Å and Au–N$_{av}$ = 2.029(8) Å for **2**; Au–Cl = 2.261(5) Å and Au–N = 2.020(16) Å for **3**) and are comparable to the distances observed in the tetrafluoroborate salt of **1**.[23]

The crystal packing observed in **2** and **3** (Fig. 3) consists of layers (along the *bc* plane, in the case of **2**) formed by [AuCl$_2$L]$^+$ cations and PF$_6^-$ anions, interacting with each other by means of weak

Table 1 Crystal data and details of the structure determination for **2** and **3**

	2	**3**
Chemical formula	$C_{12}H_{12}AuCl_2F_6N_2P$	$C_{12}H_{12}AuCl_2F_6N_2O_2P$
Formula weight	597.07	629.07
Crystal system	Monoclinic	Monoclinic
Space group	$P2_1/c$	$P2/c$
a/Å	7.6946(4)	7.8169(11)
b/Å	11.6360(5)	9.0950(7)
c/Å	19.5951(10)	13.1775(15)
β/°	101.075(6)	106.175(13)
V/Å^3	1721.77(15)	899.76(18)
Z	4	2
D_c/g cm^{-3}	2.303	2.322
F(000)	1120	592
μ/mm^{-1}	9.005	8.630
Measured reflections	13947	1821
Unique reflections	3578	1821
Unique reflections [$I > 2\sigma(I)$]	3496	1782
Data/parameters	3578/274	1821/121
R^a [$I > 2\sigma(I)$]	0.047	0.077
w$R_2{}^a$ (all data)	0.122	0.212
Largest electron density peak/e Å^{-3}	2.29 (1.00 Å from Au1)	5.34 (1.22 Å from F3)
GoF^b	1.06	1.23

^{a} $R = \sum||F_o| - |F_c||/\sum|F_o|$, w$R2 = \{\sum[w(F_o^2 - F_c^2)^2]/\sum[w(F_o^2)^2]\}^{1/2}$. ^{b} GoF $= \{\sum[w(F_o^2 - F_c^2)^2]/(n-p)\}^{1/2}$ where n is the number of data and p is the number of parameters refined.

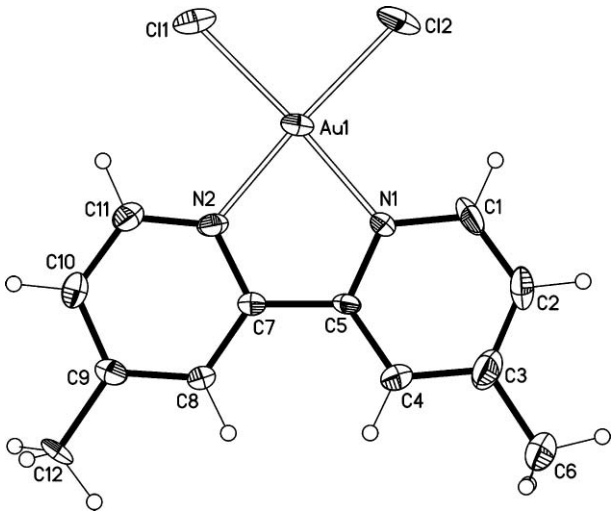

Fig. 1 ORTEP plot of **2** (the PF$_6$ anion is omitted for clarity, the ellipsoids are shown at 50% probability level).

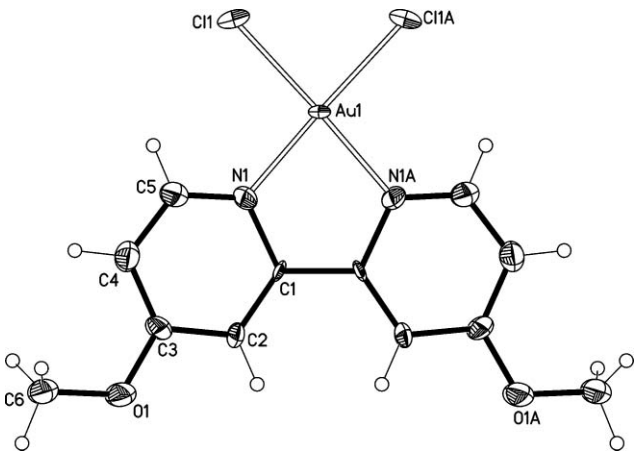

Fig. 2 ORTEP plot of **3** (the PF$_6$ anion is omitted for clarity, the ellipsoids are shown at 50% probability level). Letter A indicates symmetry generated atoms (A: $-x$, y, $0.5 - z$).

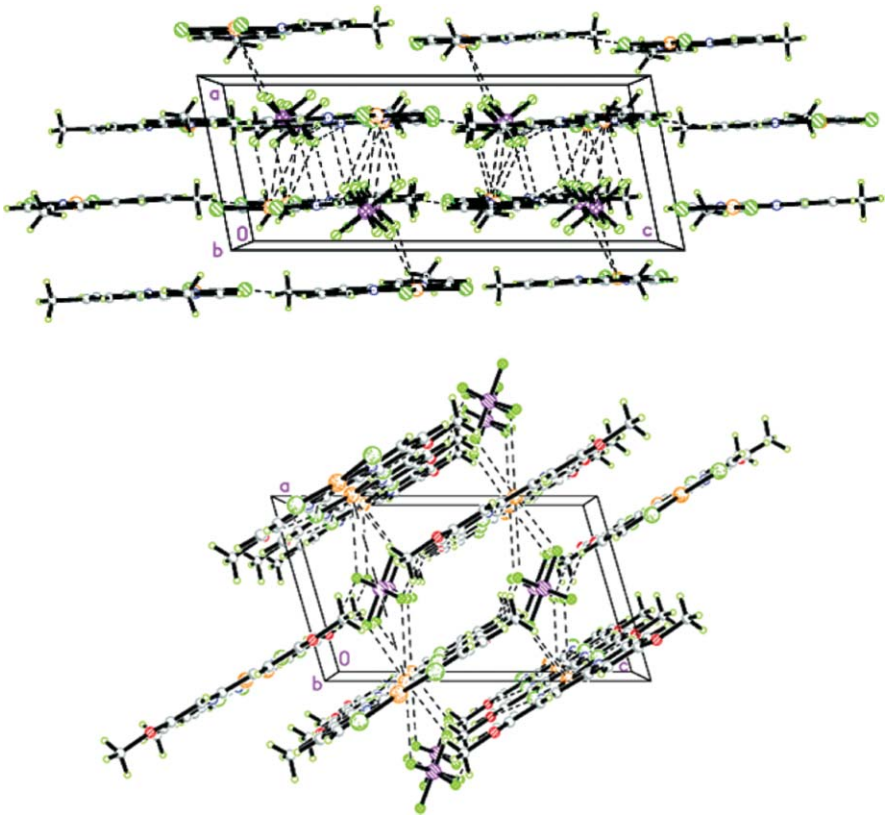

Fig. 3 Crystal packing for **2** (top) and **3** (bottom).

interactions (CH···Cl and CH···F, being 2.58 and 2.41 Å the shortest distances, respectively). These layers are linked by direct interactions between PF_6^- and the metal centre along the *a* axis (shortest Au···F distance = 2.95(3) Å for **2** and 3.25(2) Å for **3**). For **2** and **3** the *a* axis represents the shortest intermolecular distance between two metal centres, and as a consequence of the solid-state architecture, no π–π stacking between the cationic complexes is observed.

Solution studies

The solution chemistry of **1–5** was studied using spectrophotometry. The compounds were first dissolved in DMSO and the resulting solutions diluted with phosphate buffered saline (pH 7.4). Solutions were monitored over 24 h and representative spectral profiles are shown in Fig. 4 for **2**. Compounds **1–4** exhibit intense transitions in the 300–400 nm range, characteristic of the gold(III) chromophore, that may be assigned as LMCT bands.[24] For the bipyridine complexes these transitions are stable over 24 h implying that the gold(III) species is stable in solution. Only modest spectral changes are observed with time that probably corresponds to the partial hydrolysis of the chloride ligands, in accordance with ESI-MS analysis (see above). At variance with **1–4**, the dipyridylamine compound **5** was found to undergo a large, progressive increase in intensity of its major LMCT band at 320 nm that is complete within 4 h (Fig. S1, ESI†). In addition, other marked spectral changes are observed that might be ascribed to the release of the chloride and dipyridyl ligands and the formation of various degradation products. Hence, **5** was excluded from further biological screening due to its intrinsic instability in solution.

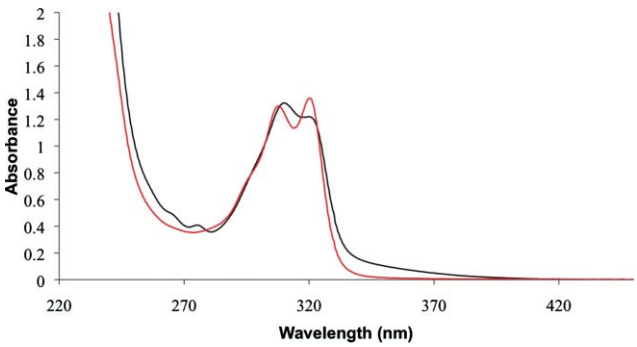

Fig. 4 UV-visible spectra of **2** (10^{-4} M) in PBS (pH 7.4) at $t = 0$ (black trace) and $t = 24$ h (red trace), incubation at 37 °C.

The reactivity of **1–4** towards biologically relevant reducing agents was evaluated spectrophotometrically. Sodium ascorbate (Asc) and glutathione (GSH) were selected as standard reducing agents. Increasing amounts of reducing agent were added to freshly prepared solutions of the compounds, as detailed in the experimental section, and UV-visible spectra were recorded. A 2 : 1 molar excess of Asc rapidly reduces all the four gold(III) compounds. Representative spectra for **2** are shown in Fig. 5. The reduction of the gold(III) centre is shown by the disappearance of the LMCT bands characteristic of the gold(III)-bipyridyl chromophore, and concomitantly, a broad absorption band appears around 620 nm that may be ascribed to the formation

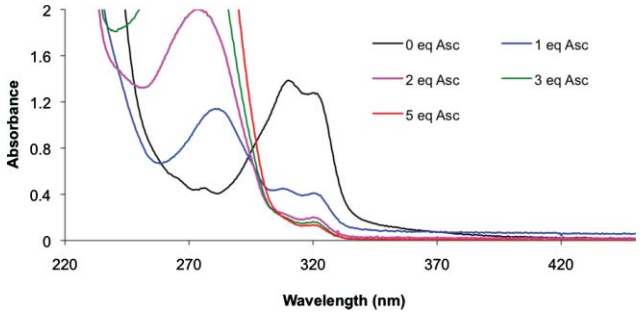

Fig. 5 UV-visible spectra of **2** (10^{-4} M) in PBS (pH 7.4) with increasing amounts of sodium ascorbate (Asc).

Table 2 IC_{50} values of **1–4** against human ovarian carcinoma cell lines sensitive (A2780) or resistant (A2780cisR) to cisplatin, compared to cisplatin. R/S = the ratio between the IC_{50} for the A2780cisR cell and the IC_{50} for the A2780 cell line

	IC_{50}/μM[a]		
Compound	A2780	A2780cisR	R/S
$[Au(bpy)Cl_2][PF_6]$ (**1**)	30.9 ± 0.6	46.0 ± 2.3	1.5
$[Au(bpMe)Cl_2][PF_6]$ (**2**)	9.8 ± 0.1	8.9 ± 0.1	0.9
$[Au(bpOMe)Cl_2][PF_6]$ (**3**)	23.4 ± 1.2	24.6 ± 2.0	1.1
$[Au(bpNH_2)Cl_2][PF_6]$ (**4**)	33.5 ± 2.0	45.0 ± 3.0	1.3
Cisplatin	4.3 ± 0.5	18.2 ± 1	4.2

[a] Mean ± SE of at least three determinations.

of colloidal gold, the final product of the reduction. Similar to Asc, GSH causes the rapid disappearance of the LMCT bands of the gold(III) centres, consistent with the idea of a reduction process (Fig. S2, ESI†), however, in contrast to the case of Asc, the formation of colloidal gold is not observed. Probably, the presence of excess glutathione favours the formation of soluble gold(I) thiolate species. Nevertheless, these results suggest that **1–4** could be reduced in an intracellular environment and that redox processes are likely to be of importance in their mechanism of action. These data are in accordance with previously reported studies on dinuclear gold(III) bipyridyl complexes.[8]

Cytotoxicity assays and biophysical studies

The antiproliferative properties of **1–4** were assayed by monitoring their ability to inhibit cell growth using the MTT assay (see Experimental section). Cytotoxic activity was determined on the human ovarian cancer (A2780) cell line, and its cisplatin-resistant variant (A2780cisR), after 72 h exposure to the compounds (see Table 2).

Compounds **1**, **3** and **4** are somewhat less cytotoxic than the cisplatin (used as a control) in the A2780 cell line whereas **2** (Table 2) has a cytotoxicity comparable to cisplatin. The lack of cross resistance for **1–4** suggests that the molecular mechanisms of cisplatin resistance[25-27] are not relevant to these gold(III) compounds suggesting a different mechanism of uptake and/or action. The most active compound of the series, **2**, contains the 4,4′-methyl-2,2′-bipyridine ligand. As mentioned above, a study on a series of 6,6′-substituted 2,2′-bipyridine oxo-bridged dinuclear gold(III) complexes showed that the introduction of methyl groups at the 6,6′-positions increases the cytotoxic potency of the molecule.[8] DFT studies indicated that the bipyridyl nitrogen atom adjacent to the methylated carbon becomes more negatively charged, increasing its donor capability.[19] According to these results the methylated derivative should have favourable electronic properties, mainly influencing the oxidising power of the gold centre, which might account for its superior cytotoxic effects. Even if the effect of methylation at the 4 and 4′ positions on the bipyridyl nitrogen is reduced,[19] it is possible that a similar effect might be in operation. However, it should be noted that the 4,4′-diamino derivative **4** is not as cytotoxic as **2**, therefore the electron donating power of the substituents may not be the only determinant of biological activity.

To gain further insights into the reactivity of **1–4** with potential biological targets, their reaction with plasmid DNA and ubiquitin (Ub, used as a model protein) was studied. Plasmid DNA was incubated with **1–4** for 24 h at 37 °C at different metal : base pair ratios ($r = 0.1$, 0.05 and 0.01) and the resulting mixtures separated by gel electrophoresis. Representative gels of pBR322 plasmid treated with **2** are displayed in Fig. 6. Notably, the migration and the quantitative distribution of the three forms of plasmid DNA (super-coiled, nicked and linear) are not affected by the presence of gold(III) complexes at any concentration, indicating that the gold compounds do not react with DNA, and contrasts markedly to the behaviour of cisplatin which interacts strongly with nucleic acids.

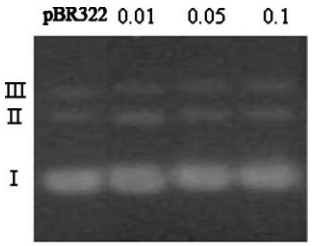

Fig. 6 Gel electrophoresis of pBR322 plasmid DNA treated with different concentrations of **2** ($r = 0.1$, 0.05 and 0.01; r = metal complex : DNA base pairs) after 24 h incubation at 37 °C. (I = super-coiled DNA; II = nicked DNA; III = linear DNA.)

The reaction of **2** with Ub was investigated by ESI-MS using an established procedure.[28,29] The compound was reacted with Ub at a 3 : 1 metal : protein molar ratio over 24 h at 37 °C. Samples were collected at various times, ultrafiltered and analysed. ESI-MS spectra for the samples (focusing on the +9 and +8 ions) after 3 and 24 h incubation are shown in Fig. 7 together with the spectrum of untreated Ub.

The resulting spectra are characterised by peaks at 952 (+9 ions) and 1071 m/z (+8 ions) characteristic of Ub and by other peaks that are attributed to protein adducts derived from **2**. Comparative analysis of the intensity of the peaks of the free protein with those of the adducts provides a qualitative indication of the degree of metalation and analysis of the peaks allows identification of the stoichiometry of the adducts and of the nature of protein bound metallic fragments. Notably, the main adduct formed by **2** [peaks at 974 (+9 ions) and 1096 m/z (+8 ions)] corresponds to protein species containing one naked gold ion (Fig. 7). The signal of this mono-adduct increases over the 24 h period. Since the bipyridyl ligand is lost on protein binding it is most likely that the gold(III) ion is reduced to gold(I). Such a phenomena has already been described for dinuclear oxo-bridged gold(III) complexes.[8,13]

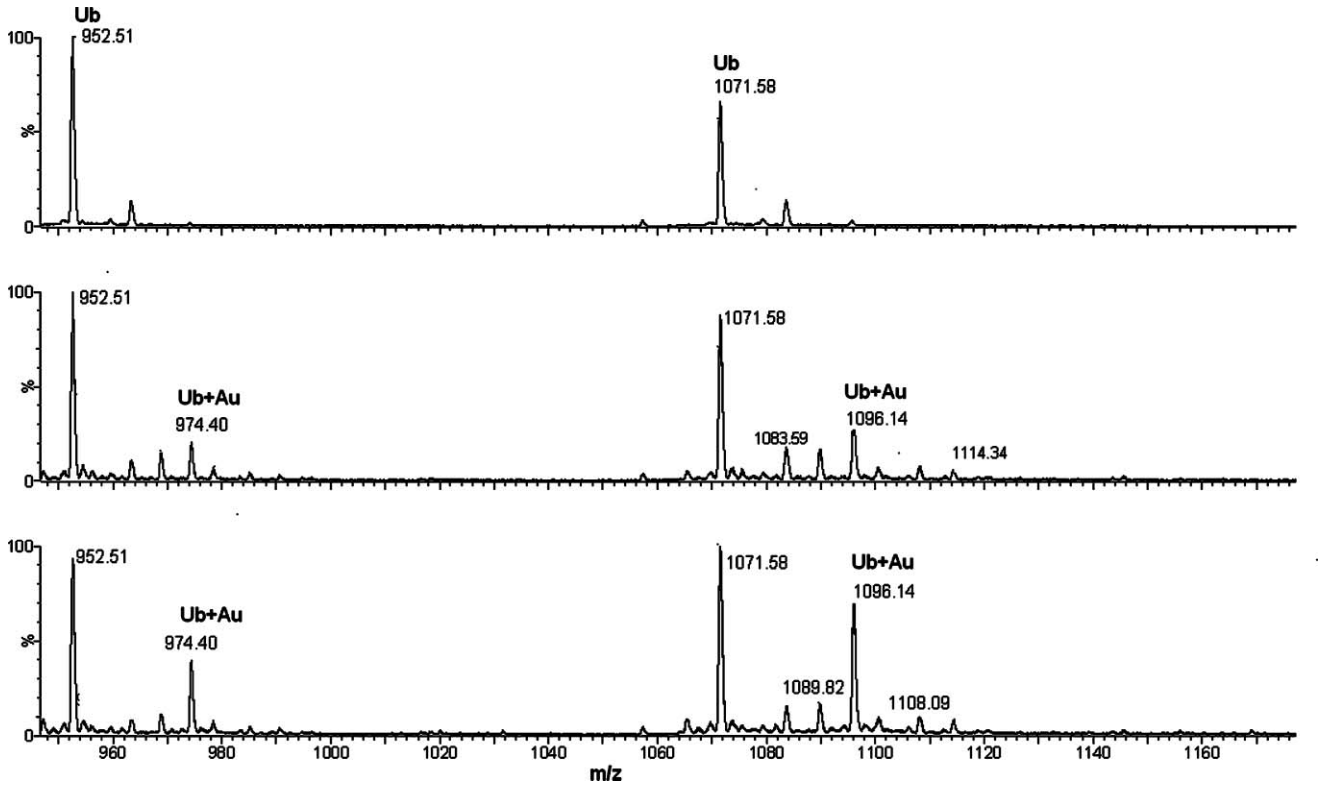

Fig. 7 ESI mass spectra (+9 and +8 ions) of Ub (top) and Ub treated with **2** (3 : 1, metal : protein ratio) in water after 3 h (middle) or 24 h incubation (bottom) at 37 °C.

Conclusions

We report here a series of novel gold(III) compounds, designed according to previously established criteria, as cytotoxic anticancer agents. Indeed, the compounds exhibit good to moderate cytotoxicities in the cancer cell lines studied, with $[Au(bpMe)Cl_2][PF_6]$ **2** being the most active (comparable to cisplatin). The substituents on the bipyridine ligands seem to play an active role in determining the chemical and biological properties of the resulting complexes. Reactions of **1–4** with plasmid DNA and Ub, analysed by gel electrophoresis and ESI-MS, respectively, demonstrate that nucleic acids are unlikely to be the pharmacological target and reactivity with amino acids seems to be favoured, also facilitating reduction of the gold centre. The possible reduction of the gold(III) ion to colloidal gold due to the interaction with biomolecules is of interest in the field of gold nanoparticles with medicinal applications.[30] This study shows that in addition to substitution of the 2,2′-bipyridine ligand at 6,6′-positions, ligand substitutions at the 4,4′-sites offers further potential for rational drug modifications.

Experimental

All starting materials were used as received from commercial sources. $NaAuCl_4$ was prepared by neutralisation of an aqueous solution of $HAuCl_4$ with Na_2CO_3. 4,4′-substituted 2,2′-bipyridine ligands were synthesised as reported[31] and dipyridin-2-yl-amine was purchased from Fluka.

^{1}H NMR spectra were recorded on a Bruker Avance II400 spectrometer at room temperature. Elemental analyses were performed on a Carlo Erba EA 1110 CHN instrument. ESI-MS spectra were obtained in acetonitrile on a Thermo Finnigan LCQ Deca XP Plus quadrupole ion-trap instrument operated in positive ion mode over a mass range of m/z 150–2000 using a literature method.[32] The ionisation energy was set at 30 V and the capillary temperature at 200 °C.

General method for the preparation of complexes 1–4

An aqueous solution of $NaAuCl_4$ (0.25 mmol, 3 mL) and solid KPF_6 (0.138 g, 0.75 mmol, excess) was added to a solution of the appropriate 2,2′-bipyridine ligand (0.25 mmol) in acetonitrile (0.5 mL). The suspension was heated to reflux for 16 h. The solution was allowed to cool at room temperature and the precipitate was filtered, washed with cold water (2 × 6 mL) and dried under vacuum. Recrystallisation from acetone–diethyl ether afforded the pure sample.

$[(bpy)AuCl_2][PF_6]$ (1). Yield: 0.137 g (96%), bright yellow powder. ^{1}H NMR (293 K, 400 MHz, $(CD_3)_2CO$): $\delta = 9.41$ (d, $^3J = 6.5$ Hz, 2 H, H^6), 8.94 (d, $^3J = 8.2$ Hz, 2 H, H^3), 8.74 (dd, $^3J = 9.0$, 6.5 Hz, 2 H, H^4), 8.15 (dd, $^3J = 6.5$, 6.5 Hz, 2 H, H^5). Anal. calculated for $C_{10}H_8AuF_6N_2OP$: C 21.11; H 1.42; N 4.92%; found: C 20.90; H 1.28; N 4.77%. ESI-MS (MeCN, positive ion mode; m/z): 423.0 $[(bpy)AuCl_2]^+$, 388 (M – Cl) and 353 (M – 2Cl).

$[(bpMe)AuCl_2][PF_6]$ (2). Yield: 0.135 g (90%), light brown powder. ^{1}H NMR (293 K, 400 MHz, $(CD_3)_2CO$): $\delta = 9.21$ (d, $^3J = 7.0$ Hz, 2 H, H^6), 8.79 (s, 2 H, H^3), 7.95 (d, $^3J = 5.4$ Hz, 2 H, H^5), 2.67 (s, 3 H, Me). Anal. calculated for $C_{12}H_{12}AuCl_2F_6N_2P$: C 24.14; H 2.01; N 4.69%; found: C 23.23; H 1.90; N 4.42%. ESI-MS

(MeCN, positive ion mode; m/z): 451.0 [(bpMe)$AuCl_2$]$^+$ (100%). Slow evaporation of **2** from acetonitrile afforded crystals suitable for structural analysis by X-ray diffraction.

[(bpOMe)$AuCl_2$][PF_6] (3). Yield: 0.125 g (83%), light yellow powder. ^{1}H NMR (293 K, 400 MHz, $(CD_3)_2CO$): $\delta = 9.12$ (d, $^3J = 7.2$ Hz, 2 H, H^6), 8.51 (d, $^4J = 2.2$ Hz, 2 H, H^3), 7.62 (dd, $^3J = 6.9$ Hz, $^4J = 2.6$ Hz, 2 H, H^5), 4.18 (s, 3H, OMe). Anal. calculated for $C_{12}H_{12}AuCl_2F_6N_2O_2P$: C 22.91; H 1.92; N 4.45%; found: C 22.41; H 1.94; N 4.36%. ESI-MS (MeCN, positive ion mode; m/z): 483.2 [(bpOMe)$AuCl_2$]$^+$ (100%). Slow evaporation of **3** from acetonitrile afforded crystals suitable for structural analysis by X-ray diffraction.

[(bpNH$_2$)$AuCl_2$][PF_6] (4). Yield: 0.147 g (82%), orange powder. ^{1}H NMR (293 K, 400 MHz, $(CD_3)_2CO$): $\delta = 8.56$ (d, $^3J = 7.2$ Hz, 2 H, H^6), 8.07 (4 H, NH_2), 7.20 (s, 2 H, H^3), 6.86 (d, $^3J = 7.2$ Hz, 2 H, H^5). Anal. calculated for $C_{10}H_{10}AuCl_2F_6N_4P$: C 20.05; H 1.68; N 9.35%; found: C 20.08; H 1.66; N 9.27%. ESI-MS (MeCN, positive ion mode; m/z): 453.3 [(bpNH$_2$)$AuCl_2$]$^+$ (100%).

Synthesis of [Au(dipyam)Cl_2][PF_6] (5)

To a solution of dipyridin-2-yl-amine (0.086 g, 0.50 mmol) in MeCN (0.5 mL) an aqueous solution of $NaAuCl_4$ (0.50 mmol, 3 mL) and solid KPF_6 (0.276 g, 1.5 mmol) was added. The suspension was stirred for 5 days at room temperature then removed by filtration. The brick red solid was washed with water (2 × 5 mL) and diethyl ether (2 × 5 mL) then dried under vacuum.

Yield: 0.24 g (82%). ^{1}H NMR (293 K, 400 MHz, $(CD_3)_2CO$): $\delta = 12.28$ (s, 1 H, NH), 8.70 (d, $^3J = 5.9$ Hz, 2 H, H^6), 8.24 (dd, $^3J = 7.3$, 6.8 Hz, 2 H, H^4), 7.57 (d, $^3J = 7.3$ Hz, 2 H, H^3), 7.52 (dd, $^3J = 6.8$, 5.9 Hz, 2 H, H^5). Anal. calculated for $C_{10}H_8AuCl_2F_6N_3P$: C 20.60; H 1.38; N 7.21%; found: C 20.26; H 1.26; N 6.92%. ESI-MS (MeCN, positive ion mode; m/z): 438 [(dipyam)$AuCl_2$]$^+$, 402.1 (M – Cl) and 367.0 (M – 2Cl).

X-Ray analysis

Data collection for **2** and **3** was performed at 140 K using Mo Kα radiation on an Oxford Diffraction Sapphire/KM4 CCD with a kappa geometry goniometer. Data were reduced using Crysalis PRO[33] and then corrected for absorption.[34] Solution and refinement for both crystal structures were performed by SHELX.[35] The structures were refined using full-matrix least-squares on F^2 with all non-hydrogen atoms anisotropically defined. Hydrogen atoms were placed in calculated positions by means of a "riding" model. Both crystals show twinning problems by reticular merohedry that have been treated in two different ways. For **2** the twinning law was identified by the new Crysalis PRO [TWIN −1 0 0 0 −1 0 1 0 1] and a BASF parameter was obtained in the last stages of refinement [BASF = 0.422(2)]. For **3** the twinning was analysed by the TWINROTMAT routine of PLATON.[36] A new HKLF5 file was then generated and used to refine the crystal structure completely, obtaining two BASF parameters [BASF1 = 0.243(6), BASF2 = 0.040(5)]. In addition, the PF_6^- anion in **2** was considerably disordered but the split model in combination with reasonable restraints (cards SIMU and DELU) resolved it successfully.

UV-visible absorption spectroscopy

The absorption spectra of the gold(III) compounds in the UV-visible region were recorded on a Perkin-Elmer Lambda 20 Bio spectrophotometer. The hydrolysis experiments were carried out with solutions of gold compounds (10^{-4} M) in PBS buffer (pH 7.4) at 37 °C by monitoring the electronic spectra of the resulting mixtures over 24 h. Moreover, the reactivity of the gold(III) complexes in the presence of Asc or GSH added in stoichiometric amount or in excess (up to 1 : 5 equivalents) was studied.

Cytotoxicity assays

Human A2780 and A2780cisR cells were obtained from the European Centre of Cell Cultures (ECACC, Salisbury, UK). All cell culture reagents were obtained from Gibco-BRL (Basel, Switzerland). Cells were grown in RPMI 1640 medium containing 10% fetal calf serum (FCS) and antibiotics. The cytotoxicity of the compounds was determined using MTT assay according to the method described by Abbey *et al.*[37] In brief, cells (100 µL) were added to a 96-well cell culture plates (Corning, NY) at the density of 25.10^3 cells per well and incubated at 37 °C for 24 h. The stock solutions of the compounds were prepared by dissolving the compounds in 1 mL of DMSO to reach a concentration of 10^{-2} M. They were then diluted in RPMI medium and added to the wells (100 µL) to obtain a final concentration ranging between 0 and 80 µM. DMSO at comparable concentrations did not show any effects on cell cytotoxicity. A negative control (RPMI medium only) and a positive control (cisplatin 50 µM) were run for all the assays. Quadruplicate cultures were established for each condition tested. After 72 h incubation at 37 °C, 20 µL of a solution of MTT (3-(4,5-dimethylthiazole-2-yl)-2,5-diphenyltetrazolium bromide) in PBS (2 mg mL^{-1}) was added to each well, and the plates were then incubated for 3 h at 37 °C. The medium was then aspirated and DMSO (100 µL) was added to dissolve the precipitate. The absorbance of each well was measured at 580 nm using a 96-well multiwell-plate reader (iEMS Reader MF, Labsystems, Bioconcept, Switzerland) and compared to the values of control cells incubated without complexes. The percentage of cell survival was then determined.

DNA electrophoresis

Samples with pBR322 plasmid DNA were prepared by adding the required volume of freshly prepared solutions of metal complexes in MilliQ water. The concentration of plasmid in the reaction mixture was 75 ng l^{-1} and the concentration of the complexes was varied to give different metal-to-base pair stoichiometries (0.1, 0.05 and 0.01). The mobility of the metal complex-treated pBR322 samples was analysed by gel electrophoresis on a 0.8% (w/v) agarose gel (Boehringer-Mannheim, Mannheim, Germany) at 90 V cm^{-1} at 25 °C for 6 h in Tris-acetate/EDTA buffer. The gel was stained for 30 min in 0.5 g ml^{-1} (w/v) ethidium bromide and the bands were analysed with a UVP gel scanner.

ESI-MS

Samples were prepared by mixing Ub 100 µM (Sigma, U6253) with an excess of the appropriate metal complex (3 : 1, metal : protein ratio) in MilliQ water and incubated over 24 h at 37 °C. Prior to

analysis, samples were extensively ultrafiltered using a Centricon YM-3 filter (Amicon Bioseparations, Millipore Corporation) in order to remove the unbound complex. ESI-MS data were acquired on a Q-Tof Ultima mass spectrometer (Waters) fitted with a standard Z-spray ion source and operated in the positive ionisation mode. Experimental parameters were set as follows: capillary voltage 3.5 kV, source temperature 80 °C, desolvation temperature 120 °C, sample cone voltage 100 V, desolvation gas flow 400 L h^{-1}, acquisition window 300–2000 m/z in 1 s. The samples were diluted 1 : 10 in water and 5 μl was introduced into the mass spectrometer by infusion at a flow rate of 20 μl min^{-1} with a solution of ACN/H_2O/HCOOH 50 : 49.8 : 0.2 (v : v : v). External calibration was carried out with a solution of phosphoric acid at 0.01%. Data were processed using the MassLynx 4.1 software.

Acknowledgements

The authors wish to thank COST D39 action for stimulating discussion. AC thanks the Swiss National Science Foundation for financial support (AMBIZIONE project no. PZ00P2_121933). SMZ and MG thank Swiss National Science Foundation for financial support. We thank Dr Michael Groessl for helping recording the MS spectra of the compounds.

References

1 S. Nobili, E. Mini, I. Landini, C. Gabbiani, A. Casini and L. Messori, *Med. Res. Rev.*, 2009, DOI: 10.1002/med.20168.
2 E. R. T. Tiekink, *Crit. Rev. Oncol. Hematol.*, 2002, **42**, 225–248.
3 X. Y. Wang and Z. J. Guo, *Dalton Trans.*, 2008, 1521–1532.
4 I. Ott, *Coord. Chem. Rev.*, 2009, **253**, 1670–1681.
5 L. Ronconi, C. Marzano, P. Zanello, M. Corsini, G. Miolo, C. Macca, A. Trevisan and D. Fregona, *J. Med. Chem.*, 2006, **49**, 1648–1657.
6 C. M. Che, R. W. Y. Sun, W. Y. Yu, C. B. Ko, N. Y. Zhu and H. Z. Sun, *Chem. Commun.*, 2003, 1718–1719.
7 R. W. Y. Sun and C. M. Che, *Coord. Chem. Rev.*, 2009, **253**, 1682–1691.
8 A. Casini, M. A. Cinellu, G. Minghetti, C. Gabbiani, M. Coronnello, E. Mini and L. Messori, *J. Med. Chem.*, 2006, **49**, 5524–5531.
9 L. Messori, G. Marcon, M. A. Cinellu, M. Coronnello, E. Mini, C. Gabbiani and P. Orioli, *Bioorg. Med. Chem.*, 2004, **12**, 6039–6043.
10 M. Coronnello, E. Mini, B. Caciagli, M. A. Cinellu, A. Bindoli, C. Gabbiani and L. Messori, *J. Med. Chem.*, 2005, **48**, 6761–6765.
11 V. Milacic, D. Fregona and Q. P. Dou, *Histol. Histopathol.*, 2008, **23**, 101–108.
12 S. Tu, R. Wai-Yin Sun, M. C. Lin, J. Tao Cui, B. Zou, Q. Gu, H. F. Kung, C. M. Che and B. C. Wong, *Cancer*, 2009, **115**, 4459–4469.
13 A. Casini, C. Hartinger, C. Gabbiani, E. Mini, P. J. Dyson, B. K. Keppler and L. Messori, *J. Inorg. Biochem.*, 2008, **102**, 564–575.
14 A. Bindoli, M. P. Rigobello, G. Scutari, C. Gabbiani, A. Casini and L. Messori, *Coord. Chem. Rev.*, 2009, **253**, 1692–1707.
15 A. Casini, G. Kelter, C. Gabbiani, M. A. Cinellu, G. Minghetti, D. Fregona, H. H. Fiebig and L. Messori, *JBIC, J. Biol. Inorg. Chem.*, 2009, **14**, 1139–1149.
16 C. Gabbiani, A. Casini and L. Messori, *Gold Bull.*, 2007, **40**, 73–81.
17 M. A. Cinellu, G. Minghetti, M. V. Pinna, S. Stoccoro, A. Zucca and M. Manassero, *J. Chem. Soc., Dalton Trans.*, 2000, 1261–1265.
18 G. Marcon, S. Carotti, M. Coronnello, L. Messori, E. Mini, P. Orioli, T. Mazzei, M. A. Cinellu and G. Minghetti, *J. Med. Chem.*, 2002, **45**, 1672–1677.
19 C. Gabbiani, A. Casini, L. Messori, A. Guerri, M. A. Cinellu, G. Minghetti, M. Corsini, C. Rosani, P. Zanello and M. Arca, *Inorg. Chem.*, 2008, **47**, 2368–2379.
20 C. M. Harris and T. N. Lockyer, *J. Chem. Soc.*, 1959, 3083–3085.
21 P. F. Shi and Q. Jiang, *Acta Crystallogr., Sect. E: Struct. Rep. Online*, 2006, **62**, M1183–M1185.
22 C. Tu, X. F. Wu, Q. Liu, X. Y. Wang, Q. Xu and Z. J. Guo, *Inorg. Chim. Acta*, 2004, **357**, 95–102.
23 E. J. L. Mcinnes, A. J. Welch and L. J. Yellowlees, *Acta Crystallogr., Sect. C: Cryst. Struct. Commun.*, 1995, **51**, 2023–2025.
24 M. A. Ivanov, M. V. Puzyk, T. A. Tkacheva and K. P. Balashev, *Russ. J. Gen. Chem.*, 2006, **76**, 165–169.
25 X. D. Yan, L. Y. Pan, Y. Yuan, J. H. Lang and N. Mao, *J. Proteome Res.*, 2007, **6**, 772–780.
26 C. A. Rabik and M. E. Dolan, *Cancer Treat. Rev.*, 2007, **33**, 9–23.
27 M. Knipp, *Curr. Med. Chem.*, 2009, **16**, 522–537.
28 A. Casini, A. Guerri, C. Gabbiani and L. Messori, *J. Inorg. Biochem.*, 2008, **102**, 995–1006.
29 C. G. Hartinger, A. Casini, C. Duhot, Y. O. Tsybin, L. Messori and P. J. Dyson, *J. Inorg. Biochem.*, 2008, **102**, 2136–2141.
30 Z. X. Wang and L. N. Ma, *Coord. Chem. Rev.*, 2009, **253**, 1607–1618.
31 S. M. Zakeeruddin, D. M. Fraser, M. K. Nazeeruddin and M. Gratzel, *J. Electroanal. Chem.*, 1992, **337**, 253–283.
32 P. J. Dyson and J. S. McIndoe, *Inorg. Chim. Acta*, 2003, **354**, 68–74.
33 O. D. Ltd., Oxford industrial Park, UK, Editon edn, 2009.
34 R. H. Blessing, *Acta Crystallogr., Sect. A: Found. Crystallogr.*, 1995, **51**, 33–38.
35 G. M. Sheldrick, *Acta Crystallogr., Sect. A: Found. Crystallogr.*, 2008, **64**, 112–122.
36 A. L. Spek, in *A Multipurpose Crystallographyc Tool*, Utrecht University, Utrecth, The Netherlands, Editon edn, 2008.
37 M. C. Alley, D. A. Scudiero, A. Monks, M. L. Hursey, M. J. Czerwinski, D. L. Fine, B. J. Abbott, J. G. Mayo, R. H. Shoemaker and M. R. Boyd, *Cancer Res.*, 1988, **48**, 589–601.